

峨眉山大火成岩省钒钛磁铁铁矿床成因研究进展

柏中杰, 钟宏, 朱维光

中国科学院 地球化学研究所, 矿床地球化学国家重点实验室, 贵阳 550081

摘要: 钒钛磁铁铁矿床主要赋存于与大火成岩省相关的镁铁-超镁铁层状岩体中, 虽然全球大火成岩省形成的镁铁-超镁铁层状岩体众多, 但大规模的钒钛磁铁铁矿成矿作用并不常见。峨眉山大火成岩省内带的攀西地区赋存有数个超大型钒钛磁铁铁矿床, 是全球最大的钒钛磁铁铁矿集区。钒钛磁铁铁矿大规模的成矿与母岩浆成分和磁铁铁矿的成因机制密切相关。此外, 形成巨厚的钒钛磁铁铁矿层还需要高效的富集机制。本文系统总结了上述几个方面的研究进展, 分析了导致钒钛磁铁铁矿大规模成矿的主要控制因素, 指出钒钛磁铁铁矿床下一步研究值得关注的问题。

关键词: 峨眉山大火成岩省; 钒钛磁铁铁矿床; 关键控制因素; 母岩浆成分

中图分类号: P611 doi: 10.19658/j.issn.1007-2802.2023.42.101

Progresses of studies on the genesis of Fe-Ti oxide deposits in the Emeishan Large Igneous Province

BAI Zhong-jie, ZHONG Hong, ZHU Wei-guang

State Key Laboratory of Ore Deposit Geochemistry, Institute of Geochemistry, Chinese Academy of Sciences, Guiyang 550081, China

Abstract: Fe-Ti oxide deposits are mainly hosted in mafic-ultramafic layered intrusions associated with Large Igneous Provinces (LIPs). Although there are many mafic-ultramafic layered intrusions formed in large igneous provinces around the world, the large-scale Fe-Ti oxide mineralization occurred in those intrusions is not common. Several layered mafic-ultramafic intrusions in the Panzihua-Xichang region, located in the inner zone of the Emeishan LIP (ELIP), hosted several world-class Fe-Ti oxide deposits, making the Panzihua-Xichang area to be the largest Fe-Ti ore province in the world. The large-scale mineralization of Fe-Ti oxides is closely related to the composition of parent magma and the enrichment mechanism of Fe-Ti oxides. Furthermore, a very effective enrichment mechanism is needed to explain how such thick Fe-Ti oxide layers were formed in these intrusions. In this paper, we have systematically reviewed recent advances of researches in the aforementioned areas, have analyzed the critical factors controlling the large-scale mineralization of Fe-Ti oxides, and have pointed out some remaining issues that should be addressed in future researches.

Key words: Emeishan large igneous province; Fe-Ti oxide deposit; critical controlling factors; parental magma composition

0 引言

钒钛磁铁铁矿床提供了全球98%的钒、92%的钛以及大量的铁(宋谢炎等, 2018), 同时还伴生有铬、钴、镍、钨等重要的战略性关键金属, 是全球最重要的

矿床类型之一。钒钛磁铁铁矿床主要赋存于与大火成岩省相关的镁铁-超镁铁层状岩体(如南非Bushveld杂岩体和我国攀枝花钒钛磁铁铁矿床)和古老的斜长岩套中(如挪威的Tellnes矿床和我国的大庙铁矿), 主要

收稿编号: 2023-147, 2023-6-28 收到, 2023-7-13 改回

基金项目: 国家自然科学基金资助项目(42122024, 42121003)

第一作者简介: 柏中杰(1983—), 男, 博士, 研究员, 获第19届侯德封奖, 研究方向: 幔源岩浆成矿作用。E-mail: baizhongjie@vip.gyig.ac.cn.

引用此文:

柏中杰, 钟宏, 朱维光. 2024. 峨眉山大火成岩省钒钛磁铁铁矿床成因研究进展. 矿物岩石地球化学通报, doi: 10.19658/j.issn.1007-2802.2023.42.101

Bai Z J, Zhong H, Zhu W G. 2024. Progresses of studies on the genesis of Fe-Ti oxide deposits in the Emeishan Large Igneous Province. Bulletin of Mineralogy, Petrology and Geochemistry, doi: 10.19658/j.issn.1007-2802.2023.42.101

金属矿物包括钛铁矿和钛铁矿,是幔源玄武质岩浆在地壳浅部岩浆房中分异演化的产物。全球由地幔柱活动形成了数量众多的大火成岩省,但钒钛磁铁矿的成矿作用在不同地区存在显著差别,仅有少数镁铁-超镁铁层状岩体产出有大型钒钛磁铁矿矿床。例如,格林兰岛的Skaergaard岩体,在岩浆演化过程中虽然出现了磁铁矿和钛铁矿的结晶,但最终并未形成具有经济价值的钒钛磁铁矿矿层(Thy et al., 2009; Tegner and Cawthorn, 2010)。南非著名的Bushveld杂岩体的上部带虽然形成了多达32层的钒钛磁铁矿层,但总厚度仅约20 m,且大多数矿层的厚度都小于1 m(Tegner et al., 2006)。而中国峨眉山大火成岩省中的攀枝花钒钛磁铁矿矿床,尽管其成矿岩体的规模远小于全球其他层状岩体,但其形成的块状矿层的厚度却超过了60 m,浸染状矿层的厚度更是达到了数百米(Pang et al., 2010)。近年来,玄武质岩浆在地壳浅部岩浆房中的分异演化过程以及与层状岩体的形成和钒钛磁铁矿成矿作用之间的关系得到了深入研究,并取得了大量的创新性认识。但是,关于钒钛磁铁矿大规模成矿的关键控制因素以及形成超大型钒钛磁铁矿矿床的动力学机制等关键问题,一直未得到很好解决。

中国峨眉山大火成岩省内带的攀西(攀枝花-西昌)地区分布有数个赋存超大型钒钛磁铁矿矿床的镁铁-超镁铁层状岩体(如攀枝花、红格、白马、太和、新街岩体等),其钒钛磁铁矿成矿作用在全球首屈一指,是全球最重要的钒钛磁铁矿矿集区。这一系列钒钛磁铁矿矿床规模大、品位高,是全球研究大火成岩省钒钛磁铁矿成矿作用的理想对象。此外,不同成矿岩体中钒钛磁铁矿矿层在赋存位置、围岩类型以及金属矿物组合等方面都存在诸多差异,从而为多角度深入研究玄武质岩浆分异演化过程与钒钛磁铁矿矿床成因提供了独特的有利条件。本文系统回顾了近年来对峨眉山大火成岩省钒钛磁铁矿矿床的母岩浆成分、矿床成因机制以及富集的动力学过程等方面的研究进展,分析了导致钒钛磁铁矿大规模成矿的主要控制因素,以期对完善钒钛磁铁矿成矿理论提供参考。

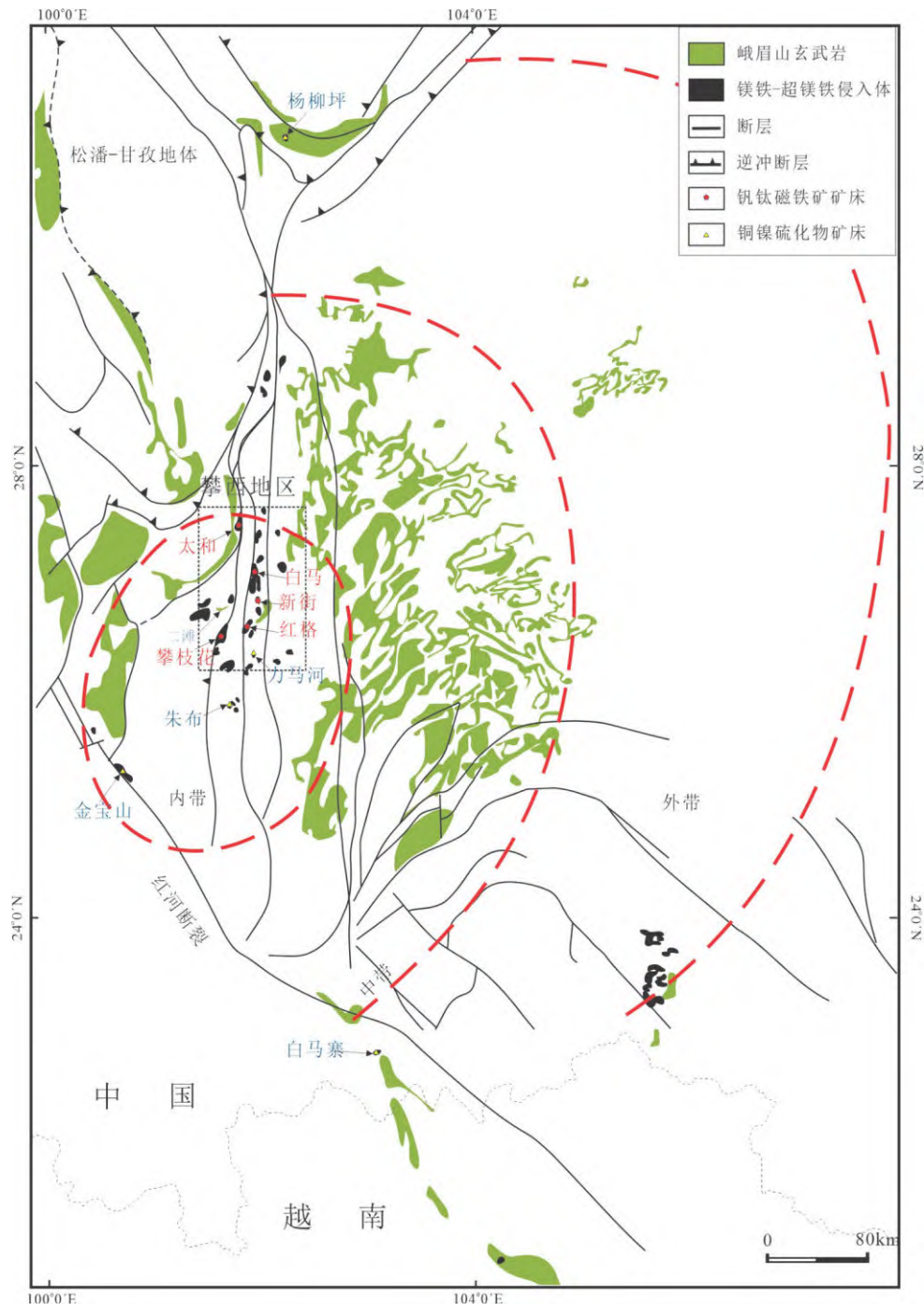
1 峨眉山大火成岩省及钒钛磁铁矿矿床地质背景

峨眉山大火成岩省形成于约260 Ma,主要分布于中国西南部的云贵川桂等省和越南北部,面积约为50万 km²(图1),主要由在短时间内喷发或就位的火山岩及其时空关系密切的侵入岩组成(Chung and Jahn, 1995; Xu et al., 2001; Zhou et al., 2002; Xiao et al.,

2004)。火山岩主要由溢流玄武岩和少量苦橄岩、火山碎屑岩以及流纹岩和粗面岩组成,厚度从大火成岩省西部的5 km到东部的几百米不等(Chung and Jahn, 1995)。根据地球化学组成,峨眉山玄武岩可分为高钛(Ti/Y > 500)和低钛(Ti/Y < 500)两个系列,前者被认为是地幔深部低程度部分熔融形成,而后者是地幔浅部较高程度部分熔融的产物(Xu et al., 2001; Xiao et al., 2004)。大火成岩省被分为内带、中带和外带,溢流玄武岩主要出露于中带和外带。内带的大部分溢流玄武岩由于后期隆升而被剥蚀(Xu and He, 2007),仅有零星的玄武岩出露于镁铁-超镁铁层状岩体附近,例如攀枝花岩体附近的二滩玄武岩和红格与新街岩体附近的龙肘山玄武岩等。后期隆升剥蚀也使得内带的侵入岩广泛出露地表。这些深成岩体主要由镁铁-超镁铁层状岩体和与之密切共生的花岗岩和正长岩组成,并与附近的玄武岩共同构成三位一体的岩石组合(图2)。

峨眉山大火成岩省中出露的含矿镁铁-超镁铁岩体可分为两类:一类是赋存铜镍硫化物矿床的岩席状或岩脉状小型岩体,在大火成岩省的内带和外带皆有分布,如力马河、金山、朱布、白马寨、杨柳坪等(图1);另一类是赋存超大型钒钛磁铁矿矿床的层状镁铁-超镁铁岩体,主要出露于大火成岩省内带的攀西地区,明显受南北向断裂控制,包括攀枝花、红格、白马、太和、新街和务本等(图2)。全球其它主要层状岩体(如Bushveld杂岩体, Skaergaard侵入体, Muskox侵入体, Kiglapait侵入体)中钒钛磁铁矿层通常赋存于岩体上部,且岩体中大多数岩性带仅含有低于20%的铁钛氧化物矿物。攀西地区这些成矿岩体的厚度仅为1~2 km,岩体规模远小于全球其它岩体。然而,其块状矿层(>50%铁钛氧化物)的厚度达60~100 m(Pang et al., 2010),并含有数百米厚的浸染状矿层(20%~50%的铁钛氧化物)(图3)。这些成矿岩体主要侵位于中元古界会理群变质沉积-火山岩及新元古界震旦系灯影组灰岩中,通常表现出明显的岩性分带和韵律层理(图3)。富矿层位主要位于各岩性带的中下部。具体到各个韵律层,矿层又赋存于韵律层的中下部。而各韵律层之间则是愈下部的韵律层矿石的富集程度越高(李德惠和茅燕石, 1982; 卢记仁等, 1988)。成矿岩体中铁钛氧化物的平均含量高达37%,远高于全球其他层状岩体(Bai et al., 2021)。攀西地区钒钛磁铁矿矿床的总储量高达72亿吨Fe₂O₃、约5.6亿吨TiO₂和约0.17亿吨V₂O₃(马玉孝等, 2003; Zhong et al., 2005),是全球最大的钒钛磁铁矿矿集区。

根据成分差异,这些成矿岩体总体上可分为两类:一类为以辉长岩为主的基性岩体,包括攀枝花、白



审图号GS(2022)4307号

图1 峨眉山大火成岩省玄武岩及钒钛磁铁矿与岩浆硫化物矿床成矿岩体分布图(据Zhou et al., 2002)

Fig.1 Distribution of basalts and mafic-ultramafic layered intrusions hosting Fe-Ti oxide deposits and mafic-ultramafic sills hosting Ni-Cu-(PGE) sulfide deposits in the Emeishan Large Igneous Province (after Zhou et al., 2002)

马和太和等岩体;另一类是含有橄辉岩-辉石岩等岩相带的基性-超基性岩体,典型的成矿岩体包括红格和新街等(刘伏等,1985;卢记仁等,1987)。此外,这些岩体的铁钛氧化物矿物组成也不尽相同。攀枝花等岩体主要矿层的铁钛氧化物矿物以磁铁矿为主,具有低的Ti/Fe和高的V/Ti比值(Pang et al., 2008a, 2008b);而红格和务本等岩体的主要矿层还含有更多的钛铁矿,

具有高的Ti/Fe比值和低的V/Ti比值(Bai et al., 2014, 2019b)。岩体中通常还含有少量的磁黄铁矿、镍黄铁矿和黄铜矿等岩浆硫化物矿物,然而仅有新街岩体显示出铂族元素矿化(Zhong et al., 2004)。

2 成矿岩体母岩浆组成及其多样性

镁铁-超镁铁层状岩体被视为研究玄武质岩浆分

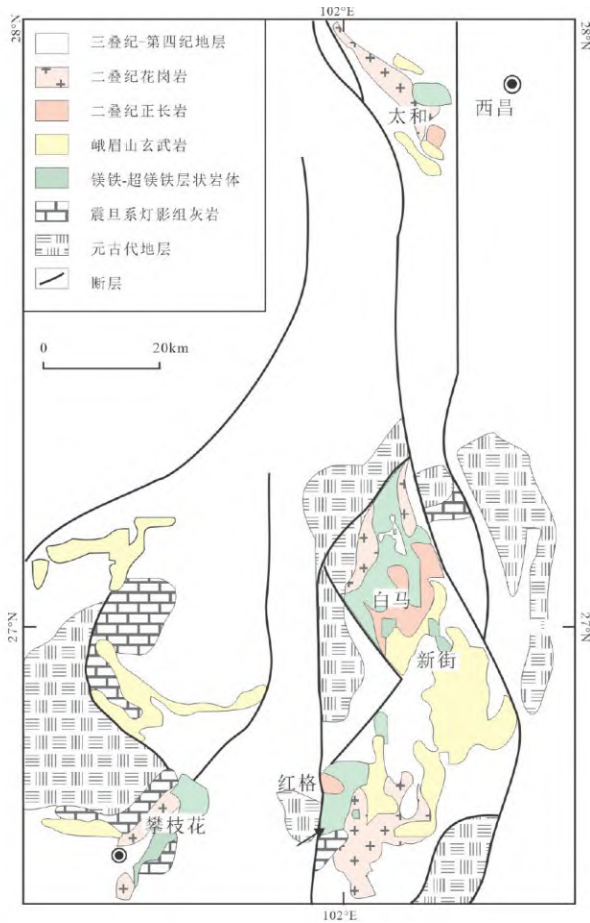


图2 攀西地区钒钛磁铁矿成矿岩体与共生酸性岩体及峨眉山玄武岩分布简图(据刘秋等,1985)

Fig.2 Simplified geological map showing the distribution of the Fe-Ti oxide mineralized intrusions and associated felsic plutons and the Emeishan basalts (after Liu et al., 1985)

异演化与成矿作用的天然实验室。获取准确的母岩浆组成是研究镁铁-超镁铁层状岩体岩浆演化、岩浆房过程以及成矿机制的重要基础,因此一直受到广大学者的高度关注。然而由于镁铁-超镁铁层状岩体经历了广泛的矿物堆晶作用,其全岩地球化学成分体现的是堆晶矿物组合与粒间熔体不同比例的混合,并不能真实反映母岩浆成分,因此需要通过其他手段来估算成矿岩体的母岩浆成分。岩体边缘带快速冷却结晶的冷凝边或矿物中的熔体包裹体通常被认为能够直接记录层状岩体的母岩浆成分(Spandler et al., 2000; Barnes et al., 2010; Jakobsen et al., 2010; Wilson, 2012; Maier et al., 2016),而与层状岩体时空关系密切的岩脉或玄武岩也被认为能够近似代表层状岩体母岩浆组成(Cawthorn et al., 1981; Jakobsen et al., 2010)。此外,通过分析结晶矿物的元素含量并结合相应的分配系数或精确估算堆晶矿物及粒间熔体的比例并结合全岩微量元素也可间接估算母岩浆成分(Bédard, 1994; God-

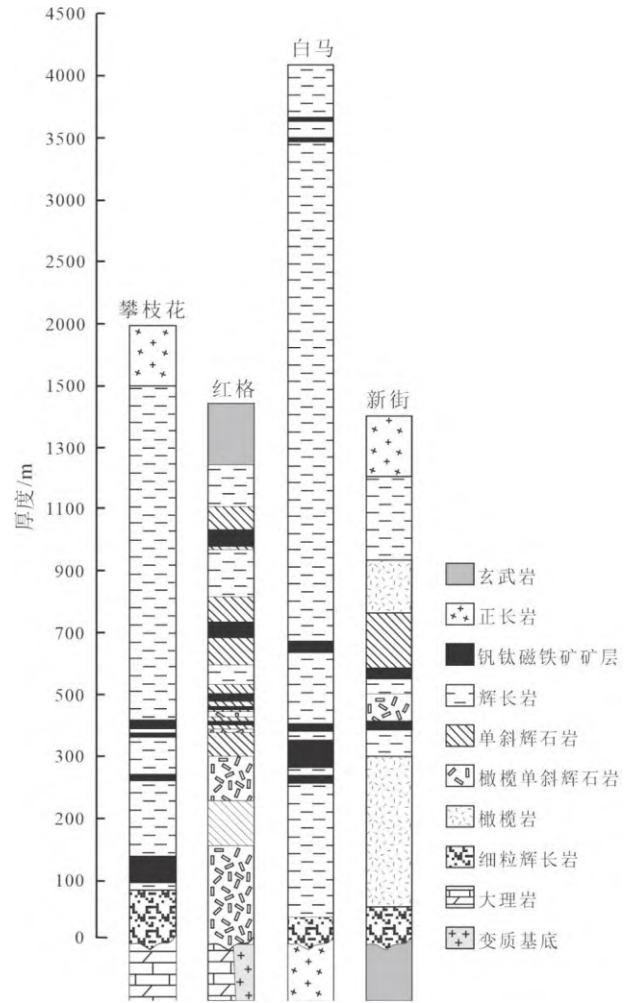


图3 攀西地区钒钛磁铁矿成矿岩体岩性柱状简图 (据Pang et al., 2010)

Fig.3 Idealized stratigraphic columns of the Fe-Ti oxide mineralized intrusions in the Panzhihua-Xichang area (after Pang et al., 2010)

el et al., 2011; Bai et al., 2014; Yang et al., 2019)。全球学者通过上述方法对层状岩体的母岩浆成分开展了大量研究并取得了丰硕成果,从而推动了层状岩体的研究。例如,不同学者通过边缘带获取了Bushveld杂岩体不同岩相带的母岩浆成分(例如B-1, B-2, B-3; Harmer and Sharpe, 1985; Sharpe and Hulbert, 1985; Barnes et al., 2010),为深入研究其铬铁矿、PGE以及钒钛磁铁矿成矿机制奠定了基础。

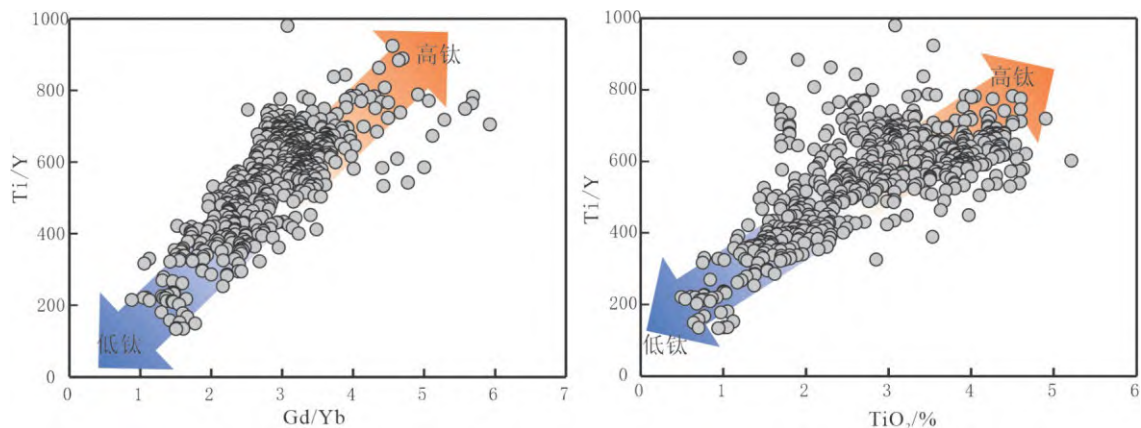
由于峨眉山大火成岩省中这些层状岩体大规模钒钛磁铁矿成矿作用,一般都认为其母岩浆为富集Fe、Ti的玄武质岩浆,与峨眉山高钛玄武岩的成分类似(Zhong et al., 2005; Zhou et al., 2008; Pang et al., 2010; Bai et al., 2012; Song et al., 2013)。但是峨眉山玄武岩的成分从高钛到低钛几乎连续变化,其中高钛玄武岩自身就具有很大的成分变化范围。例如,高钛玄武岩的TiO₂含量可以从2%至5%不变(图4),这意味

着目前还不清楚何种Ti含量的玄武岩能够代表成矿岩体的母岩浆成分。Pang等(2008a)使用接近最高TiO₂含量(4.85%)的峨眉山玄武岩来模拟攀枝花矿床铁钛氧化物的结晶过程。Song等(2013)以峨眉山高钛苦橄岩橄榄石斑晶中的熔体包裹体成分作为原始岩浆进行分离结晶模拟,发现经过约50%的分离结晶将形成富铁钛玄武质岩浆(TiO₂=4.9%)。而Zhou等(2005)通过对每个岩相带成分加权平均,获得了更为富铁钛的全岩成分。而Zhang等(2009)推测攀枝花岩体母体岩浆成分与辉长岩(PZH-1)成分接近,含有高达~17% TFeO。相反,Ganino等(2008)在他们的岩石学模型中使用了含有较低的TiO₂含量的玄武岩(TiO₂=2.6%)。与此类似,Howarth和Prevec(2013)对不同TiO₂含量玄武岩的结晶分异过程进行了对比模拟,发现接近高钛玄武岩TiO₂含量下限的玄武质岩浆能够很好重现攀枝花岩体中所观察到的矿物成分和结晶顺序。Bai等(2019a)认为,攀枝花岩体的边缘带细粒辉长岩是岩浆侵入岩浆房后与围岩接触,发生了快速冷却固结的产物,因此能够近似代表母岩浆成分。他们的研究进一步发现细粒辉长岩的成分与岩体附近的二滩玄武岩基本类似,并接近高钛玄武岩低TiO₂端元。

尽管不同学者对成矿岩体母岩浆成分的估算存在明显差异,但都显示出相对富铁钛的成分特征。这种较为富铁钛的母岩浆为大规模成矿奠定了物质基础。研究发现,高钛玄武质岩浆很难由橄榄岩地幔部分熔融形成(Prytulak and Elliott, 2007)。目前对于这种相对富铁钛母岩浆的成因主要有几种观点:①来自富铁钛的辉石岩地幔源区(Zhang et al., 2009; Hou et al., 2011, 2012);②地幔柱-俯冲洋壳相互作用过程中溶解了俯冲洋壳中的铁钛氧化物(Bai et al., 2014);③深

部岩浆房橄榄石等硅酸盐矿物的广泛分离结晶(Song et al., 2013; She et al., 2014);④深部岩浆房经过液态不混溶形成的富铁熔体(Zhou et al., 2005, 2013)。值得注意的是,相对富铁钛的母岩浆广泛存在于全球其他大火成岩省,然而并没有都形成大规模的钒钛磁铁矿矿床,这可能意味着母岩浆相对较高的铁钛含量并非最终能否成矿的关键因素。例如,格林兰Skaergaard岩体的母岩浆同样含有高达3%的TiO₂和15%的TFeO(Nielsen, 2004)(图5),在岩浆演化过程中也形成了相当量的磁铁矿和钛铁矿矿物,但是并没有有效聚集并形成大规模的钒钛磁铁矿矿床。作为铁苦橄岩的典型代表,Pechenga绿岩带相关镁铁-超镁铁岩体也没有展现出良好的钒钛磁铁矿成矿潜力(图5)。与此相反,南非Bushveld杂岩体上部带的钒钛磁铁矿矿层的母岩浆仅含有1.0%的TiO₂和11.7%的TFeO(Tegner et al., 2006),并不具有富集铁钛的特征。

近年来的研究发现,这些成矿岩体的母岩浆成分还存在明显的差异。尽管母岩浆成分并非成矿与否的关键因素,但这种差异可能导致了成矿的多样性。Bai等(2014)对比了红格岩体和攀枝花岩体含矿层位单斜辉石的主微量成分,发现红格岩体母岩浆较攀枝花岩体具有更高的TiO₂含量。实验岩石学研究表明,钛铁矿的饱和和结晶主要受岩浆TiO₂含量控制,与氧逸度关系不大(Toplis and Carroll, 1995)。红格母岩浆较高的钛含量更有利于钛铁矿的饱和,因此形成磁铁矿+钛铁矿的金属矿物组合,而攀枝花母岩浆钛含量较低,钛铁矿很难直接饱和,因此形成的金属矿物以磁铁矿为主。此外,太和岩体的钒钛磁铁矿层还含有大量磷灰石,因此She等(2014, 2015)提出太和岩体母岩浆具有较高的磷含量。其原因可能是成矿岩浆在深部岩浆房溶解了磷灰石,而



数据引自GEOROC数据库(<http://georoc.mpch-mainz.gwdg.de/georoc>)

图4 峨眉山大火成岩省玄武岩组成呈连续型变化

Fig. 4 Diagrams showing the continuous compositional change of basalts in the Emeishan Large Igneous Province

后侵入太和岩浆房后同时结晶铁钛氧化物和磷灰石。

3 钒钛磁铁矿成因模式

尽管近年来对峨眉山大火成岩省镁铁-超镁铁层状岩体中钒钛磁铁矿矿床开展了大量研究,但其成因机制仍存在较大争议。目前主要的成因观点大体可归纳为以下三类:①铁钛氧化物矿物在深部岩浆房内结晶,然后以晶粥形式侵位到当前岩浆房后成矿(Ho-warth et al.,2013);②由玄武质岩浆液态不混溶形成的富铁熔体形成(Zhou et al.,2005;Dong et al.,2013;Wang and Zhou,2013;Liu et al.,2014a;Wang et al.,2018);③直接从玄武质母岩浆中结晶后经过重力分异或流动分异形成(Ganino et al.,2008;Pang et al.,2008a,2008b;Bai et al.,2012,2016;Song et al.,2013;Luan et al.,2014)。

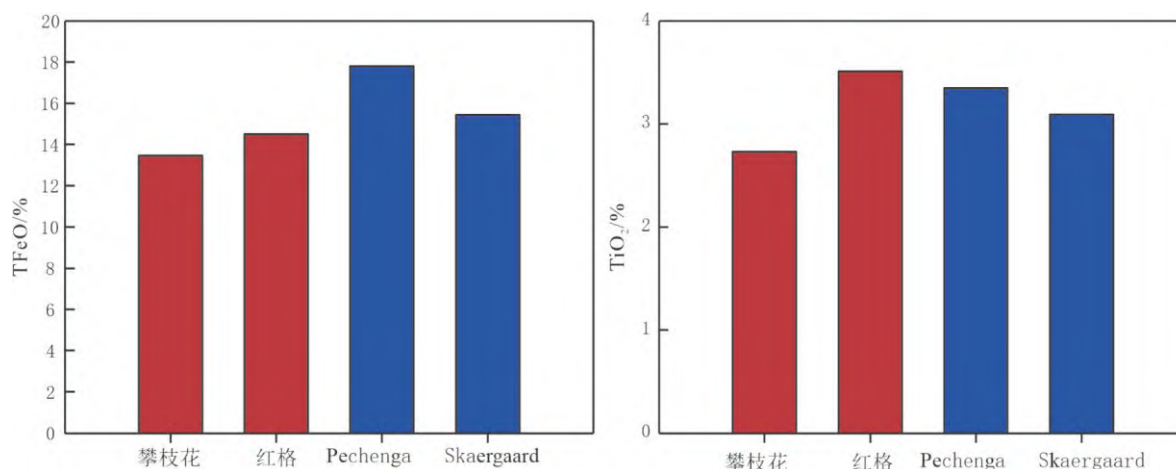
3.1 深部晶粥侵位模型

关于形成镁铁-超镁铁层状岩体的岩浆是以晶粥还是纯岩浆的形式侵位的争议由来已久(Latypov,2009;Marsh,2013)。越来越多的研究发现,至少在部分岩体中,岩浆是以晶粥的形式侵位的。其典型的地球化学特征是由晶粥形成的堆晶矿物及全岩成分在垂向上保持稳定。此外,晶粥与残余岩浆结晶的矿物成分具有明显差异,表现出多压结晶(polybaric crystallization)的特征(Charlier et al.,2009,2010)。这一模型也被用来解释一些矿床中矿体规模与成矿岩浆金属含量之间表现出的明显质量不平衡现象,即大量金属矿物在深部岩浆房结晶,然后随岩浆以晶粥的形式转移到浅部岩浆房继而发生沉淀。例如,一些研究认为南非Bushveld岩体中的铬铁矿层即是通过这一机制形成

(Eales,2000;Mondal and Mathez,2007;Voordouw et al.,2009;Eales and Costin,2012)。该模式也被Ho-warth等(2013)用来解释攀枝花岩体中主要钒钛磁铁矿矿层的成因。事实上,这些成矿岩体的母岩浆相对苦橄质原始岩浆较为演化,因此被认为在深部还存在一个更为基性的岩浆房(Bai et al.,2012;Song et al.,2013;Wang et al.,2014)。攀枝花岩体边缘带中粗粒橄榄石即被认为是随岩浆从深部岩浆房转移到当前岩浆房的产物(Bai et al.,2019a)。然而铁钛氧化物具有较硅酸盐岩矿物更高的密度和铬铁矿更粗的粒度,更可能是在高位岩浆房中原位结晶形成。事实上,峨眉山玄武岩和苦橄岩中的斑晶主要为橄榄石、普通辉石和斜长石,基本不含铁钛氧化物斑晶(Xu et al.,2001;Xiao et al.,2004;Zhang et al.,2006;Kamenetsky et al.,2012)。

3.2 液态不混溶

液态不混溶模型认为,随着玄武质岩浆的分异演化,熔体将变得不稳定从而发生不混溶现象,形成共存的富Fe-Ti-P熔体和富Si-Al-Na-K熔体。这一现象已被证实广泛存在于拉斑玄武岩和一些碱性和钙碱性火山岩的分异演化过程之中(Philpotts,1978,1982)。自岩浆液态不混溶模式提出以来,不断有矿床学家尝试用铁玄武质熔体不混溶作用形成的富铁熔体来解释包括峨眉山大火成岩省相关钒钛磁铁矿矿床在内的全球各地钒钛磁铁矿矿床的成因(Bateman,1951;Lister,1966;Reynolds,1985;Von Gruenewaldt,1993;Zhou et al.,2005,2013;Namur et al.,2012;Wang and Zhou,2013)。该模式认为,硅酸盐岩浆在演化过程中熔离出的富铁熔体通过下沉作用或压滤作用堆积在岩体的一



数据来源:Hanski and Smolkin,1995;Nielsen,2004;Bai et al.,2012,2019a

图5 攀枝花与红格岩体与Pechenga和Skaergaard岩体母岩浆TFeO和TiO₂含量对比

Fig.5 Comparison of the TFeO and TiO₂ contents of parental magmas for the Panzhihua, Hongge, Pechenga and Skaergaard intrusions

定部位而形成矿床。该模式能够在一定程度上解释整合和不整合产出的纯氧化物矿体的地质现象,因而受到一些学者的欢迎。例如,Zhou等(2005)提出攀枝花矿床的块状矿层是由不混溶的富铁氧化物熔体直接形成。后续不同学者针对成矿岩体的岩石显微结构和熔体包裹体开展了大量研究(Dong et al., 2013; Wang and Zhou, 2013; Liu et al., 2014a; Wang et al., 2018),特别是发现这些熔体包裹体在成分上具有富铁贫硅和富硅贫铁的两个端元,因此认为攀西地区的层状岩体发生了广泛的岩浆液态不混溶作用,并导致了钒钛磁铁矿的大规模成矿。此外,一些研究发现成矿岩体中Mg、Fe同位素在铁钛氧化物与硅酸盐矿物之间存在明显的不平衡,这被认为是存在液态不混溶作用的证据(Liu et al., 2014b; Cao et al., 2019),不过也有研究认为这是铁钛氧化物与硅酸盐矿物亚固相再平衡的结果(Chen et al., 2014)。

然而,液态不混溶模式在解释钒钛磁铁矿床成因时也遇到了一定的争议与挑战。首先,尽管液态不混溶在玄武岩中被广泛地观察到,但仅以微小的玻璃质熔滴存在于玄武岩基质中或者呈熔体包裹体出现在深成岩体的硅酸盐和磷灰石矿物中,说明其很可能只是粒间熔体尺度的晚期液态不混溶。因此,在层状岩体中,液态不混溶形成的富铁与富硅液滴能否有效地合并并且大尺度分离形成宏观上各自独立的熔体层还有待证实。其次,液态不混溶形成的富铁熔体将同时富磷,而层状岩体中的块状钒钛磁铁矿矿石几乎是由磁铁矿和钛铁矿组成,仅含有少量的硅酸盐矿物,特别是很多块状矿石中几乎不含磷灰石。

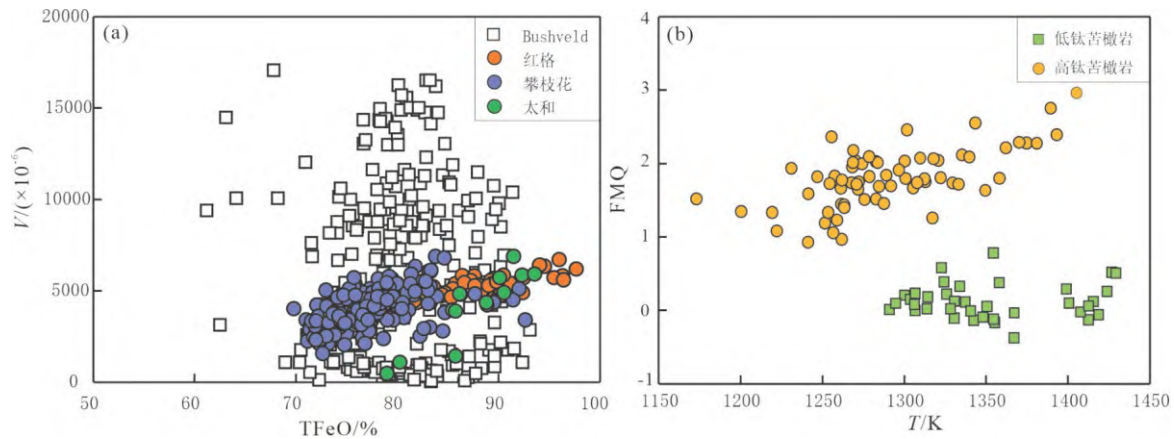
3.3 结晶分异

除岩浆不混溶模式之外,更多学者倾向于认为铁钛氧化物直接从玄武质岩浆中结晶而来,其中最为典型的是重力结晶分异模式。这一经典模式最早由Wager和Brown(1968)提出,以此来解释层状岩体中普遍存在的韵律旋回,其也被用于解释钒钛磁铁矿床的形成(Emslie, 1975; Goldberg, 1984; McLelland et al., 1994; Eales and Cawthorn, 1996; Dymek and Owens, 2001; Tegner et al., 2006; Charlier et al., 2006; Tollari et al., 2008)。在玄武质岩浆演化过程中,由于同时结晶的铁钛氧化物矿物及硅酸盐矿物之间的密度差异,相对较重的铁钛氧化物矿物具有更高的沉积速率,在适当的情况下下沉到底部形成氧化物矿层。这一机制与一些层状岩体中磁铁矿层与下部围岩突变而与上覆围岩渐变过渡的接触关系相吻合。近来的研究发现成矿岩体的底部呈现出显著的凹凸不平,岩浆房底部的凹陷将进一步促使晶粥发生流动分

异,从而更有利于形成块状富铁矿层(Song et al., 2013)。结晶分异能够很好的解释与围岩整合产出的层状矿体的矿物组成和矿物成分的垂向变化,但少部分呈脉状、透镜状、席状、网脉状矿体并不能简单的归因于重力结晶分异。

在对攀西地区钒钛磁铁矿床研究过程中,大家发现铁钛氧化物开始出现时的共生矿物组合具有较全球其他矿床更高的基性程度,如橄榄石 $Fo > 71$,单斜辉石 $Mg^{\#} > 80$ 和斜长石 $An > 69$ (Pang et al., 2009; Bai et al., 2012, 2016),结合其主要赋矿层位于岩体中下部这一不同于全球其他层状岩体的地质特征,认为钒钛磁铁矿是在玄武质岩浆分异演化的较早阶段结晶出来。目前对于导致磁铁矿早期结晶的原因还没有定论。部分学者认为富铁钛的母岩浆是促使磁铁矿从玄武质岩浆中较早结晶的主要因素(Zhang et al., 2009; Song et al., 2013)。导致母岩浆富铁钛的原因包括来自富铁钛的辉石岩地幔源区、铁钛氧化物的溶解以及深部岩浆房硅酸盐矿物的分离结晶。部分钒钛磁铁矿床中出现了较多的角闪石(例如红格; Luan et al., 2014),指示其成矿母岩浆可能含有较高的水含量。岩浆中较高的水含量将抑制硅酸盐矿物特别是斜长石的结晶而对铁钛氧化物影响不大,从而导致铁钛氧化物的较早结晶。更多的研究发现变价元素V在这些矿床的磁铁矿矿物中的分配系数较低(图6a),表明磁铁矿是从较为氧化的岩浆中结晶出来(Pang et al., 2010; Bai et al., 2012; She et al., 2015)。实验岩石学研究表明,在铁玄武质岩浆体系中,氧逸度的变化对铁钛氧化物的结晶温度和相对时间起着明显的控制作用(Toplis and Carroll, 1995; Botcharnikov et al., 2008)。碳酸盐围岩的混染被认为是导致成矿母岩浆氧逸度升高的首要因素(Ganino et al., 2008)。但是Yu等(2015)通过O-Sr-Nd同位素发现这些岩体的碳酸盐混染比例很低,并不足以导致岩浆的氧逸度明显升高。Bai等(2019)发现,峨眉山高钛苦橄岩与低钛苦橄岩的氧逸度具有明显的差异,其中高钛苦橄岩的氧逸度与成矿母岩浆具有相似的较高的氧逸度,因此认为成矿母岩浆的高氧逸度继承自地幔源区(图6b)。而这种氧化的地幔源区可能与地幔柱-新特提斯洋俯冲板片的相互作用有关(Bai et al., 2022)。峨眉山大火成岩省氧逸度的不均一性也被后续研究所证实(Cao and Wang, 2022; Wu et al., 2022)。

需要指出的是,结晶分异过程被认为广泛存在于包括Bushveld杂岩体,Skaergaard岩体以及峨眉山大火成岩省相关钒钛磁铁矿床在内的典型层状岩体的成岩过程中,同时在这些岩体的岩浆演化过程中也



磁铁矿数据引自Ashwal et al.,2005; Pang et al.,2008b; Shellnutt and Pang, 2012; Song et al.,2013; Yuan et al.,2017; Fischer,2018; Bai et al.,2021; 氧逸度数据据Bai et al.,2019

图6 (a)攀西地区钒钛磁铁矿成矿岩体与Bushveld杂岩体磁铁矿V含量及(b)峨眉山高钛和低钛苦橄岩氧逸度
Fig.6 (a) Vanadium contents in titanomagnetites of the intrusions in the Panzhihua–Xichang area and the Bushveld Complex and (b) the oxygen fugacities of the Emeishan high-Ti and low-Ti picrite samples

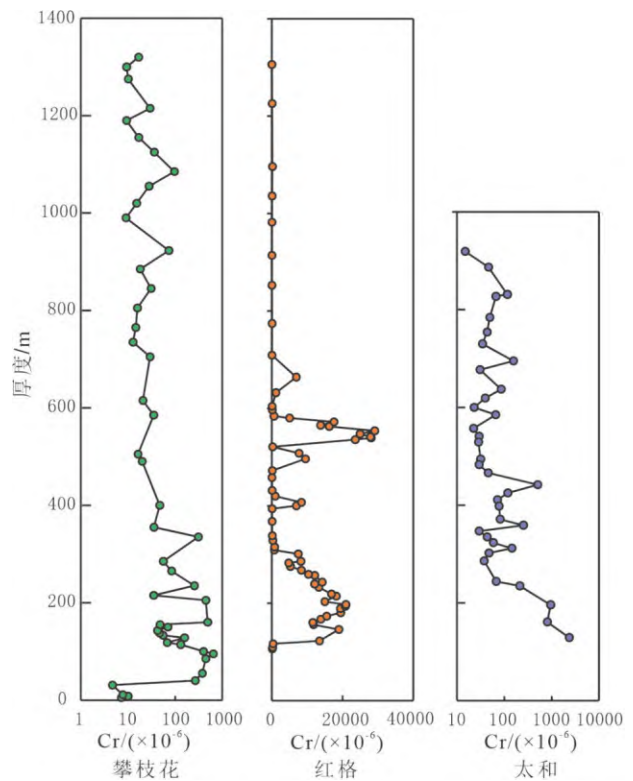
被认为发生了岩浆的液态不混溶作用。然而这些岩体中钒钛磁铁矿成矿规模却呈现明显差异。由此可见,除了重力结晶分异和液态不混溶等岩浆过程之外,还有其他特殊的机制在富集成矿过程中起了重要的作用。

4 钒钛磁铁矿富集过程

相比全球其他镁铁-超镁铁层状岩体,峨眉山大火成岩省中这些钒钛磁铁矿成矿岩体最显著的特征是其巨厚的块状矿层和侵染状矿层(图3)。其全岩铁钛氧化物的平均含量为>30%,是全球其他著名层状岩体的近2倍(Tegner et al., 2009; Thy et al., 2009; Yuan et al., 2017)。同时也是实验测定的钒钛磁铁矿在铁玄武质岩浆中共结比例的2倍(Thy and Lofgren, 1994; Toplis and Carroll, 1995; Botcharnikov et al., 2008)。开放的岩浆通道系统被认为是导致钒钛磁铁矿高效富集成矿的主要因素。

4.1 多期岩浆周期性补充

如果岩浆房是一个封闭的岩浆系统,那么玄武质母岩浆侵入岩浆房后,从中结晶出的矿物成分将呈现出与结晶分异趋势一致的规律性变化。Skaergaard岩体即是这样的典型实例,其矿物成分(例如斜长石An, 橄榄石Fo和辉石Wo-En)从岩体的底部到顶部逐渐降低(McBirney, 1989)。然而峨眉山大火成岩省中这些含矿层状岩体往往显示出复杂的岩石及化学组成变化(图7),因此与简单的单次岩浆侵入后的结晶分异规律并不一致,而是呈现出开放岩浆系统的特征。Zhong等(2003)对红格岩体的全岩组成分析结果表明,微量元素比值在各旋回边界出现了相应的反转。进一步研



数据来源: Bai et al., 2021; Chen et al., 2017; She et al., 2015

图7 攀西地区钒钛磁铁矿成矿岩体磁铁矿Cr含量变化柱状图

Fig.7 Diagrams for variations of Cr contents in magnetites from various Fe-Ti oxide mineralized intrusions in the Panzhihua-Xichang area

究发现红格及攀枝花岩体中硅酸盐矿物成分以及磁铁矿中Cr、Ni等相容元素含量呈现出逐渐降低与突然反转升高的周期性变化(Pang et al., 2009; Bai et al.,

2012; Song et al., 2013; Chen et al., 2017), 这些特征都表明在层状岩体形成过程中经历了多期次的岩浆补充叠加。白马、太和等层状岩体也表现出相似的特征 (Liu et al., 2014c; She et al., 2015), 说明峨眉山大火成岩省中这些钒钛磁铁矿成矿岩体普遍经历了多期岩浆侵入。新的岩浆补给不仅提供额外的能量, 改变岩浆的分异过程, 还会结晶出更多的铁钛氧化物, 有利于厚层状矿石的形成。新岩浆注入岩浆房还可能导致流动分异作用, 在岩浆流动过程中, 铁钛氧化物与硅酸盐矿物之间由于密度差异将发生分选作用, 密度大的铁钛氧化物沉淀聚集在密度轻的硅酸盐之下形成矿层 (Song et al., 2013)。此外, 新注入的基性岩浆与演化的残余岩浆的混合将有利于岩浆中S的饱和熔离, 为层状岩体中伴生的Co、Ni等关键金属的富集创造了条件。

4.2 岩浆通道系统

理论上, 层状岩体各岩相带加权平均后的总体成分应该与玄武质母岩浆成分接近, 因此岩体的总体成分往往也被用来反映层状岩体的母岩浆成分 (Nielsen, 2004)。然而系统的研究发现峨眉山大火成岩省中这些层状岩体的总体成分与玄武质母岩浆成分相去甚远。例如Bai等(2012)发现红格岩体相对玄武质岩浆普遍高度亏损不相容元素(例如Nb、Ta、Zr、Hf等), 同时具有明显低的硅和高的铁钛含量 (Bai et al.,

2021)(图8), 说明形成层状岩体的岩浆并未完全保留在成矿岩浆房中。研究还发现, 岩体附近共生的正长岩/花岗岩具有高硅、低铁钛和富集不相容元素特征, 与层状岩体成分特征形成互补 (Shellnutt et al., 2009; Shellnutt and Jahn, 2010), 因此认为这些共生的酸性岩体代表了形成基性层状岩体的玄武质岩浆分异演化晚期的残余岩浆。模拟计算表明玄武质岩浆大约需要经历超过70%~80%的结晶分异才能演化到中酸性岩浆成分。这一比例与Namur等(2011)关于Sept Iles岩体顶部A型酸性岩石是由玄武质岩浆经过大约90%结晶分异产生的结论一致。而Vantongerren等(2010)则估计玄武质岩浆通过结晶分异形成Bushveld岩体主带上部和上部带, 并产生了大约15%~25%的酸性岩浆且已离开岩浆房。然而质量平衡计算结果表明即使加入30%的正长岩组分后的总体成分相对玄武质母岩浆仍具有明显低的硅和高的铁钛含量(图8)。显然共生酸性岩体还不足以完全平衡岩体成分, 即还存在抽出岩浆房的其他组分。除酸性岩之外, 这些成矿岩体附近还分布着具有较低铁含量的峨眉山玄武岩 (Bai et al., 2012)。因此研究提出成矿岩体是玄武质岩浆向上运移的岩浆通道, 这些玄武岩是在下部成矿岩浆房结晶, 并卸载了大量密度重的磁铁矿后喷出地表的残余岩浆 (Bai et al., 2012; 陈列锰等, 2014; 宋谢炎等,

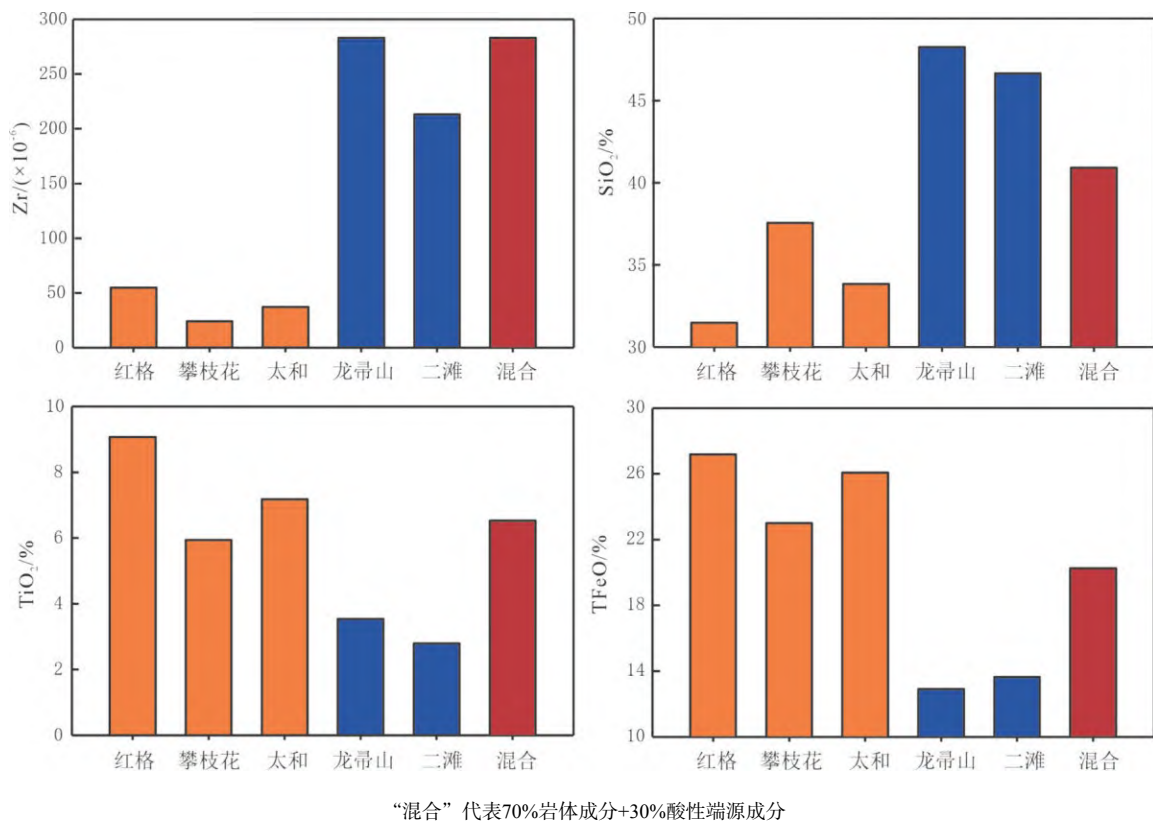


图8 成矿岩体全岩成分与峨眉山高钛玄武岩成分对比

Fig.8 Comparison of the bulk compositions of the mineralized intrusions and those of the coeval Emeishan high-Ti basalts

2018)(图9)。事实上, Tao等(2015)对峨眉山大火成岩省玄武岩、苦橄岩中斑晶结晶时的温压计算结果显示, 岩浆自壳幔边界—中地壳—上地壳从高温到低温逐级演化形成多级岩浆房储运系统, 镁铁-超镁铁层状岩体是岩浆通道系统的表现。同时, 这些玄武岩的单斜辉石等硅酸盐矿物斑晶中含有铁钛氧化物包裹体, 说明这些斑晶是在成矿岩浆房与铁钛氧化物共结并随玄武质岩浆抽离至地表。而高密度的铁钛氧化物保留在成矿岩浆房, 从而导致了铁钛矿化物的富集成矿(Bai et al., 2021)。

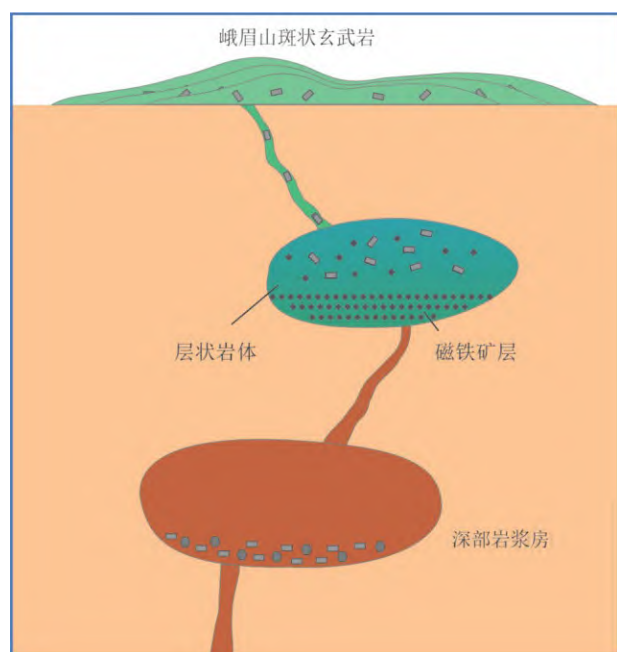


图9 钒钛磁铁矿岩浆通道成矿模式图

Fig.9 Schematic model of the magmatic conduit system for the Fe-Ti oxide mineralization

5 问题与展望

近二十年来, 峨眉山大火成岩省相关钒钛磁铁矿矿床吸引了国内外学者的广泛关注。不同学者从各个角度对这些矿床进行了深入研究, 在母岩浆成分、磁铁矿成因机制和富集过程等方面取得了显著进展, 但仍存在一些亟待解决的重要问题。以往研究多从地球化学角度对单个矿床进行详细解剖, 但针对成矿物质运移、聚集的物理过程的研究相对薄弱。例如结晶分异过程中密度不同的共结矿物在动态岩浆房中的迁移、聚集路径及效率, 以及岩浆液态不混溶形成的富铁熔体在晶粥中如何与富硅熔体分离并向下渗滤等。此外, 针对性开展实验岩石学研究, 厘清母岩浆成分、氧逸度、挥发分等因素在岩浆演化过程中的作用将有助于加深对层状岩体相关钒钛磁铁矿成矿作用的理解。

峨眉山大火成岩省中已发现的超大型钒钛磁铁矿矿床主要位于内带的攀西地区, 而其他地区的成矿潜力如何尚不清楚。氧逸度与钒钛磁铁矿成矿作用关系密切, 近年来的研究发现峨眉山大火成岩省的氧化还原状态存在明显的不均一性。因此, 厘清大火成岩省氧逸度的时空变化规律及其主要控制因素对评估钒钛磁铁矿成矿潜力具有重要意义。钒钛磁铁矿矿床不仅是Fe、Ti、V的主要来源, 同时还伴生了Cr、Co、Ni、Sc等大量的关键金属。尽管其含量较低, 但其总体规模相当可观。因此, 查明这些伴生关键金属在矿床中的赋存状态和富集机制, 进而评估其资源潜力不仅具有重要的科学意义, 更具有明显的经济价值。

作者贡献声明: 柏中杰, 研究构思和设计、数据收集、撰写稿件初稿; 钟宏、朱维光, 参与文章重要章节的写作和修改; 柏中杰、钟宏, 提供基金支持。

利益冲突声明: 作者保证本文无利益冲突。

致谢: 感谢侯通教授在审稿过程中提出的宝贵意见。

参考文献 (References):

- Ashwal L D. 2005. Magmatic stratigraphy in the Bushveld Northern Lobe: Continuous geophysical and mineralogical data from the 2950 m Bellevue drillcore. *South African Journal of Geology*, 108(2): 199–232
- Bai Z J, Zhong H, Hu R Z, Zhu W G, Hu W J. 2019. Composition of the chilled marginal rocks of the Panzhihua layered intrusion, Emeishan large igneous province, SW China: Implications for parental magma compositions, sulfide saturation history and Fe-Ti oxide mineralization. *Journal of Petrology*, 60(3): 619–648
- Bai Z J, Zhong H, Hu R Z, Zhu W G. 2021. World-class Fe-Ti-V oxide deposits formed in feeder conduits by removing cotectic silicates. *Economic Geology*, 116(3): 681–691
- Bai Z J, Zhong H, Li C S, Zhu W G, Hu W J. 2016. Association of cumulus apatite with compositionally unusual olivine and plagioclase in the Taihe Fe-Ti oxide ore-bearing layered mafic-ultramafic intrusion: Petrogenetic significance and implications for ore genesis. *American Mineralogist*, 101(10): 2168–2175
- Bai Z J, Zhong H, Li C, Zhu W G, He D F, Qi L. 2014. Contrasting parental magma compositions for the hongge and Panzhihua magmatic Fe-Ti-V oxide deposits, Emeishan large igneous province, SW China. *Economic Geology*, 109(6): 1763–1785
- Bai Z J, Zhong H, Naldrett A J, Zhu W G, Xu G W. 2012. Whole-rock and mineral composition constraints on the genesis of the giant hongge Fe-Ti-V oxide deposit in the Emeishan large igneous province, southwest China. *Economic Geology*, 107(3): 507–524
- Bai Z J, Zhong H, Zhu W G, Hu W J, Chen C J. 2019. The genesis of the newly discovered giant Wuben magmatic Fe-Ti oxide deposit in the Emeishan Large Igneous Province: A product of the late-stage redistribution and sorting of crystal slurries. *Mineralium Deposita*, 54(1): 31–46
- Bai Z J, Zhong H, Zhu W G, Hu W J. 2022. Mantle plume-subducted oceanic slab interaction contributes to geochemical heterogeneity of the Emeishan

- large igneous province. *Chemical Geology*, 611: 121117
- Barnes S J, Maier W D, Curl E A. 2010. Composition of the marginal rocks and sills of the rustenburg layered suite, bushveld complex, South Africa: Implications for the formation of the platinum-group element deposits. *Economic Geology*, 105(8): 1491–1511
- Bateman A M. 1951. The formation of late magmatic oxide ores. *Economic Geology*, 46(4): 404–426
- Bédard J H. 1994. A procedure for calculating the equilibrium distribution of trace elements among the minerals of cumulate rocks, and the concentration of trace elements in the coexisting liquids. *Chemical Geology*, 118(1–4): 143–153
- Botcharnikov R E, Almeev R R, Koepke J, Holtz F. 2008. Phase relations and liquid lines of descent in hydrous ferrobasalt—Implications for the skaergaard intrusion and Columbia River flood basalts. *Journal of Petrology*, 49(9): 1687–1727
- Cao Y H, Wang C Y, Huang F, Zhang Z F. 2019. Iron isotope systematics of the Panzihua mafic layered intrusion associated with giant Fe-Ti oxide deposit in the Emeishan large igneous province, SW China. *Journal of Geophysical Research (Solid Earth)*, 124(1): 358–375
- Cao Y H, Wang C Y. 2022. Contrasting oxidation states of low-Ti and high-Ti magmas control Ni-Cu sulfide and Fe-Ti oxide mineralization in Emeishan Large Igneous Province. *Geoscience Frontiers*, 13(6): 101434
- Charlier B, Duchesne J C, Vander Auwera J, Storme J Y, Maquil R, Longhi J. 2010. Polybaric fractional crystallization of high-alumina basalt parental magmas in the egersund-ogna massif-type anorthosite (rogaland, SW Norway) constrained by plagioclase and high-alumina orthopyroxene megacrysts. *Journal of Petrology*, 51(12): 2515–2546
- Charlier B, Duchesne J C, Vander Auwera J. 2006. Magma chamber processes in the Tellnes ilmenite deposit (Rogaland Anorthosite Province, SW Norway) and the formation of Fe-Ti ores in massif-type anorthosites. *Chemical Geology*, 234(3–4): 264–290
- Charlier B, Namur O, Duchesne J C, Wiszniewska J, Parecki A, Auwera J V. 2009. Cumulate origin and polybaric crystallization of Fe-Ti oxide ores in the suwalki anorthosite, northeastern Poland. *Economic Geology*, 104(2): 205–221
- Chen L M, Song X Y, Hu R, Yu S Y, He H J, She Y W, Dai Z, Xie W. 2016. Revision 2 1 2 Controls on trace element partitioning among co-crystallizing 3 minerals: Evidence from the Panzihua layered intrusion, SW China. *American Mineralogist*, 102(5): 1006–1020
- Chen L M, Song X Y, Zhu X K, Zhang X Q, Yu S Y, Yi J N. 2014. Iron isotope fractionation during crystallization and sub-solidus re-equilibration: Constraints from the Baima mafic layered intrusion, SW China. *Chemical Geology*, 380: 97–109
- 陈列猛, 易俊年, 宋谢炎, 于宋月, 余宇伟, 甄炜, 栾燕, 向建新. 2014. 峨眉山大火成岩省内带黑谷田含钒钛磁铁矿层状岩体成因. *岩石学报*, 30(5): 1415–1431 [Chen L M, Yi J N, Song X Y, Yu S Y, She Y W, Xie W, Luan Y, Xiang J X. 2014. Petrogenesis of the Heigutian Ti-V-magnetite ore-bearing layered intrusion, the inner zone of the Emeishan large igneous province. *Acta Petrologica Sinica*, 30(5): 1415–1431 (in Chinese with English abstract)]
- Chung S L, Jahn B M. 1995. Plume-lithosphere interaction in generation of the Emeishan flood basalts at the Permian-Triassic boundary. *Geology*, 23(10): 889
- Dong H, Xing C M, Wang C Y. 2013. Textures and mineral compositions of the Xinjie layered intrusion, SW China: Implications for the origin of magnetite and fractionation process of Fe-Ti-rich basaltic magmas. *Geoscience Frontiers*, 4(5): 503–515
- Dymek R F. 2001. Petrogenesis of apatite-rich rocks (nelsonites and oxide-apatite gabbroanorthosites) associated with massif anorthosites. *Economic Geology*, 96(4): 797–815
- Eales H V, Cawthorn R G. 1996. The bushveld complex. In: *Developments in Petrology*. Amsterdam: Elsevier: 181–229
- Eales H V, Costin G. 2012. Crustally contaminated komatiite: Primary source of the chromitites and marginal, lower, and critical zone magmas in a staging chamber beneath the bushveld complex. *Economic Geology*, 107(4): 645–665
- Eales H V. 2000. Implications of the chromium budget of the Western Limb of the Bushveld Complex. *South African Journal of Geology*, 103(2): 141–150
- Emslie R F. 1975. Nature and origin of anorthositic suites. *Geoscience Canada*, 2(2): 17–124
- Fischer L. 2018. The upper zone of the bushveld complex, South Africa: Parental magma and crystallization processes. PhD Thesis, Gottfried Wilhelm Leibniz Universität Hannover, Hannover, 129
- Ganino C, Arndt N T, Zhou M F, Gaillard F, Chauvel C. 2008. Interaction of magma with sedimentary wall rock and magnetite ore genesis in the Panzihua mafic intrusion, SW China. *Mineralium Deposita*, 43(6): 677–694
- Godel B, Barnes S J, Maier W D. 2011. Parental magma composition inferred from trace element in cumulus and intercumulus silicate minerals: An example from the Lower and Lower Critical Zones of the Bushveld Complex, South-Africa. *Lithos*, 125(1–2): 537–552
- Goldberg S A. 1984. Geochemical relationships between anorthosite and associated iron-rich rocks, Laramie Range, Wyoming. *Contributions to Mineralogy and Petrology*, 87(4): 376–387
- Grant Cawthorn R, Davies G, Clublely-Armstrong A, McCarthy T S. 1981. Sills associated with the Bushveld Complex, South Africa: An estimate of the parental magma composition. *Lithos*, 14(1): 1–16
- Hanski E J, Smolkin V F. 1995. Iron- and LREE-enriched mantle source for early Proterozoic intraplate magmatism as exemplified by the Pechenga ferropicrites, Kola Peninsula, Russia. *Lithos*, 34(1–3): 107–125
- Harmer R E, Sharpe M R. 1985. Field relations and strontium isotope systematics of the marginal rocks of the eastern Bushveld Complex. *Economic Geology*, 80(4): 813–837
- Hou T, Zhang Z C, Pirajno F. 2012. A new metallogenic model of the Panzihua giant V-Ti-iron oxide deposit (Emeishan Large Igneous Province) based on high-Mg olivine-bearing wehrlite and new field evidence. *International Geology Review*, 54(15): 1721–1745
- Hou T, Zhang Z C, Ye X R, Encarnacion J, Reichow M K. 2011. Noble gas isotopic systematics of Fe-Ti-V oxide ore-related mafic-ultramafic layered intrusions in the Panxi area, China: The role of recycled oceanic crust in their petrogenesis. *Geochimica et Cosmochimica Acta*, 75(22): 6727–6741
- Howarth G H, Prevec S A, Zhou M F. 2013. Timing of Ti-magnetite crystallisation and silicate disequilibrium in the Panzihua mafic layered intrusion: Implications for ore-forming processes. *Lithos*, 170–171: 73–

89

- Howarth G H, Prevec S A. 2013. Hydration vs. oxidation: Modelling implications for Fe-Ti oxide crystallisation in mafic intrusions, with specific reference to the Panzihua intrusion, SW China. *Geoscience Frontiers*, 4(5): 555–569
- Jakobsen J K, Tegner C, Brooks C K, Kent A J R, Lesher C E, Nielsen T F D, Wiedenbeck M. 2010. Parental magma of the Skaergaard intrusion: Constraints from melt inclusions in primitive troctolite blocks and FG-1 dykes. *Contributions to Mineralogy and Petrology*, 159(1): 61–79
- Kamenetsky V S, Chung S L, Kamenetsky M B, Kuzmin D V. 2012. Picrites from the Emeishan large igneous province, SW China: A compositional continuum in primitive magmas and their respective mantle sources. *Journal of Petrology*, 53(10): 2095–2113
- Latypov R. 2009. Testing the validity of the petrological hypothesis ‘No phenocrysts, No post-emplacement differentiation’. *Journal of Petrology*, 50(6): 1047–1069
- Lister G F. 1966. The composition and origin of selected iron-titanium deposits. *Economic Geology*, 61(2): 275–310
- Liu P P, Zhou M F, Chen W T, Boone M, Cnudde V. 2014. Using multiphase solid inclusions to constrain the origin of the Baima Fe-Ti-(V) oxide deposit, SW China. *Journal of Petrology*, 55(5): 951–976
- Liu P P, Zhou M F, Luais B, Cividini D, Rollion-Bard C. 2014. Disequilibrium iron isotopic fractionation during the high-temperature magmatic differentiation of the Baima Fe-Ti oxide-bearing mafic intrusion, SW China. *Earth and Planetary Science Letters*, 399: 21–29
- Liu P P, Zhou M F, Wang C Y, Xing C M, Gao J F. 2014. Open magma chamber processes in the formation of the Permian Baima mafic-ultramafic layered intrusion, SW China. *Lithos*, 184–187: 194–208
- 刘秋, 沈发奎, 张光宗, 张云湘. 1985. 攀西地区层状侵入体. 张云湘主编. 中国攀西裂谷文集, 地质出版社, 北京: 85–111 [Liu D, Shen F K, Zhang G Z, Zhang Y X. 1985. Stratified intrusions in Panxi area. In: Zhang Y X (Ed.). *Collected Works of the Panxi Rift Valley, China*. Geological Publishing House, Beijing: 85–110 (in Chinese)]
- 李德惠, 茅燕石. 1982. 四川攀西地区含钒钛磁铁矿层状侵入体的韵律层及形成机理. *矿物岩石*, 2(1): 29–41, 134 [Li D H, Mao Y S. 1982. Rhythm layer and formation mechanism of layered intrusions containing vanadium-bearing titanomagnetite in Panxi area, Sichuan Province. *Journal of Mineralogy and Petrology*, 2(1): 29–41, 134 (in Chinese)]
- Luan Y, Song X Y, Chen L M, Zheng W Q, Zhang X Q, Yu S Y, She Y W, Tian X L, Ran Q Y. 2014. Key factors controlling the accumulation of the Fe-Ti oxides in the Hongge layered intrusion in the Emeishan Large Igneous Province, SW China. *Ore Geology Reviews*, 57: 518–538
- 卢记仁, 张光弟, 张承信, 顾光先, 刘玉书, 黄与能. 1987. 攀西层状基性超基性岩体岩浆类型及成因. *矿床地质*, 6(2): 1–15 [Lu J R, Zhang G D, Zhang C X, Gu G X, Liu Y S, Huang Y N. 1987. Magmatic types and geneses of the layered intrusions in panzihua-xichang area. *Mineral Deposits*, 6(2): 1–15 (in Chinese with English abstract)]
- 卢记仁, 张光弟, 张承信, 顾光先, 刘玉书, 黄与能. 1988. 攀西层状岩体及钒钛磁铁矿床成因模式. *矿床地质*, 7(2): 3–11 [Lu J R, Zhang G D, Zhang C X, Gu G X, Liu Y S, Huang Y N. 1988. A genetic model for layered intrusions and vanadic titanomagnetite deposits in panzihua-xichang area. *Mineral Deposits*, 7(2): 3–11 (in Chinese with English abstract)]
- Maier W D, Barnes S J, Karykowski B T. 2016. A chilled margin of komatiite and Mg-rich basaltic andesite in the western Bushveld Complex, South Africa. *Contributions to Mineralogy and Petrology*, 171(6): 57
- Marsh B D. 2013. On some fundamentals of igneous petrology. *Contributions to Mineralogy and Petrology*, 166(3): 665–690
- 马玉孝, 纪相田, 李金成, 黄明. 2003. 攀枝花矿产资源. 成都: 成都理工大学出版社: 1–275 [Ma Y X, Ji X T, Li J C, Huang M. 2003. *Mineral resources in Panzihua*. Chengdu: Chengdu University of Technology Press: 1–275 (in Chinese)]
- McBirney A R. 1989. The skaergaard layered series: I. structure and average compositions. *Journal of Petrology*, 30(2): 363–397
- McLelland J, Ashwal L, Moore L. 1994. Composition and petrogenesis of oxide-, apatite-rich gabbro-norites associated with Proterozoic anorthosite massifs: Examples from the Adirondack Mountains, New York. *Contributions to Mineralogy and Petrology*, 116(1): 225–238
- Mondal S K, Mathez E A. 2007. Origin of the UG2 chromitite layer, bushveld complex. *Journal of Petrology*, 48(3): 495–510
- Namur O, Charlier B, Holness M B. 2012. Dual origin of Fe-Ti-P gabbros by immiscibility and fractional crystallization of evolved tholeiitic basalts in the Sept Iles layered intrusion. *Lithos*, 154: 100–114
- Namur O, Charlier B, Toplis M J, Higgins M D, Hounsell V, Liégeois J P, Vander Auwera J. 2011. Differentiation of tholeiitic basalt to A-type granite in the sept iles layered intrusion, Canada. *Journal of Petrology*, 52(3): 487–539
- Nielsen T F D. 2004. The shape and volume of the skaergaard intrusion, Greenland: Implications for mass balance and bulk composition. *Journal of Petrology*, 45(3): 507–530
- Pang K N, Li C S, Zhou M F, Ripley E M. 2008. Abundant Fe-Ti oxide inclusions in olivine from the Panzihua and Hongge layered intrusions, SW China: Evidence for early saturation of Fe-Ti oxides in ferrobaltic magma. *Contributions to Mineralogy and Petrology*, 156(3): 307–321
- Pang K N, Li C S, Zhou M F, Ripley E M. 2009. Mineral compositional constraints on petrogenesis and oxide ore genesis of the Late Permian Panzihua layered gabbroic intrusion, SW China. *Lithos*, 110(1–4): 199–214
- Pang K N, Zhou M F, Lindsley D, Zhao D G, Malpas J. 2008. Origin of Fe-Ti oxide ores in mafic intrusions: Evidence from the Panzihua intrusion, SW China. *Journal of Petrology*, 49(2): 295–313
- Pang K N, Zhou M F, Qi L, Shellnutt G, Wang C Y, Zhao D G. 2010. Flood basalt-related Fe-Ti oxide deposits in the Emeishan large igneous province, SW China. *Lithos*, 119(1–2): 123–136
- Philpotts A R. 1978. Textural evidence for liquid immiscibility in tholeiites. *Mineralogical Magazine*, 42(324): 417–425
- Philpotts A R. 1982. Compositions of immiscible liquids in volcanic rocks. *Contributions to Mineralogy and Petrology*, 80(3): 201–218
- Prytulak J, Elliott T. 2007. TiO₂ enrichment in ocean island basalts. *Earth and Planetary Science Letters*, 263(3–4): 388–403
- Reynolds I M. 1985. Contrasted mineralogy and textural relationships in the uppermost titaniferous magnetite layers of the Bushveld Complex in the Bierkraal area north of Rustenburg. *Economic Geology*, 80(4): 1027–1048
- Sharpe M R, Hulbert L J. 1985. Ultramafic sills beneath the eastern Bushveld Complex; mobilized suspensions of early lower zone cumulates in a

- parental magma with boninitic affinities. *Economic Geology*, 80(4): 849–871
- She Y W, Song X Y, Yu S Y, He H L. 2015. Variations of trace element concentration of magnetite and ilmenite from the Taihe layered intrusion, Emeishan large igneous province, SW China: Implications for magmatic fractionation and origin of Fe-Ti-V oxide ore deposits. *Journal of Asian Earth Sciences*, 113: 1117–1131
- She Y W, Yu S Y, Song X Y, Chen L M, Zheng W Q, Luan Y. 2014. The formation of P-rich Fe-Ti oxide ore layers in the Taihe layered intrusion, SW China: Implications for magma-plumbing system process. *Ore Geology Reviews*, 57: 539–559
- Shellnutt J G, Jahn B M. 2010. Formation of the Late Permian Panzhihua plutonic-hypabyssal-volcanic igneous complex: Implications for the genesis of Fe-Ti oxide deposits and A-type granites of SW China. *Earth and Planetary Science Letters*, 289(3–4): 509–519
- Shellnutt J G, Pang K N. 2012. Petrogenetic implications of mineral chemical data for the Permian Baima igneous complex, SW China. *Mineralogy and Petrology*, 106(1): 75–88
- Shellnutt J G, Zhou M F, Zellmer G F. 2009. The role of Fe–Ti oxide crystallization in the formation of A-type granitoids with implications for the Daly gap: An example from the Permian Baima igneous complex, SW China. *Chemical Geology*, 259(3–4): 204–217
- Song X Y, Qi H W, Hu R Z, Chen L M, Yu S Y, Zhang J F. 2013. Formation of thick stratiform Fe-Ti oxide layers in layered intrusion and frequent replenishment of fractionated mafic magma: Evidence from the Panzhihua intrusion, SW China. *Geochemistry, Geophysics, Geosystems*, 14(3): 712–732
- 宋谢炎, 陈列猛, 于宋月, 陶琰, 余宇伟, 栾燕, 张晓琪, 何海龙. 2018. 峨眉山大火成岩省钒钛磁铁矿床地质特征及成因. *矿物岩石地球化学通报*, 37(6): 1003–1018 [Song X Y, Chen L M, Yu S Y, Tao Y, She Y W, Luan Y, Zhang X Q, He H L. 2018. Geological features and genesis of the V-Ti magnetite deposits in the Emeishan large igneous province, SW China. *Bulletin of Mineralogy, Petrology and Geochemistry*, 37(6): 1003–1018 (in Chinese with English abstract)]
- Spandler C J, Eggins S M, Arculus R J, Mavrogenes J A. 2000. Using melt inclusions to determine parent-magma compositions of layered intrusions: Application to the Greenhills Complex (New Zealand), a platinum group minerals bearing, island-arc intrusion. *Geology*, 28(11): 991
- Tao Y, Putirka K, Hu R Z, Li C S. 2015. The magma plumbing system of the Emeishan large igneous province and its role in basaltic magma differentiation in a continental setting. *American Mineralogist*, 100(11–12): 2509–2517
- Tegner C, Cawthorn R G, Kruger F J. 2006. Cyclicity in the main and upper zones of the bushveld complex, South Africa: Crystallization from a zoned magma sheet. *Journal of Petrology*, 47(11): 2257–2279
- Tegner C, Cawthorn R G. 2010. Iron in plagioclase in the Bushveld and Skaergaard intrusions: Implications for iron contents in evolving basic magmas. *Contributions to Mineralogy and Petrology*, 159(5): 719–730
- Thy P, Leshner C E, Tegner C. 2009. The Skaergaard liquid line of descent revisited. *Contributions to Mineralogy and Petrology*, 157(6): 735–747
- Thy P, Lofgren G E. 1992. Experimental constraints on the low-pressure evolution of transitional and mildly alkalic basalts: Multisaturated liquids and coexisting augites. *Contributions to Mineralogy and Petrology*, 112(2): 196–202
- Tollari N, Barnes S J, Cox R A, Nabil H. 2008. Trace element concentrations in apatites from the Sept-Îles Intrusive Suite, Canada—Implications for the genesis of nelsonites. *Chemical Geology*, 252(3–4): 180–190
- Toplis M J, Carroll M R. 1995. An experimental study of the influence of oxygen fugacity on Fe-Ti oxide stability, phase relations, and mineral—Melt equilibria in ferro-basaltic systems. *Journal of Petrology*, 36(5): 1137–1170
- Vantongerren J A, Mathez E A, Kelemen P B. 2010. A felsic end to bushveld differentiation. *Journal of Petrology*, 51(9): 1891–1912
- Von Gruenewaldt G. 1993. Ilmenite-apatite enrichments in the upper zone of the bushveld complex: A major titanium-rock phosphate resource. *International Geology Review*, 35(11): 987–1000
- Voordouw R, Gutzmer J, Beukes N J. 2009. Intrusive origin for Upper Group (UG1, UG2) stratiform chromitite seams in the Dwars River area, Bushveld Complex, South Africa. *Mineralogy and Petrology*, 97(1): 75–94
- Wager L R, Brown G M. 1968. Layered igneous rocks. Edinburgh: Oliver and Boyd, 588
- Wang C Y, Zhou M F, Yang S H, Qi L, Sun Y L. 2014. Geochemistry of the Abulandang intrusion: Cumulates of high-Ti picritic magmas in the Emeishan large igneous province, SW China. *Chemical Geology*, 378–379: 24–39
- Wang C Y, Zhou M F. 2013. New textural and mineralogical constraints on the origin of the Hongge Fe-Ti-V oxide deposit, SW China. *Mineralium Deposita*, 48(6): 787–798
- Wang K, Wang C Y, Ren Z Y. 2018. Apatite-hosted melt inclusions from the Panzhihua gabbroic-layered intrusion associated with a giant Fe-Ti oxide deposit in SW China: Insights for magma unmixing within a crystal mush. *Contributions to Mineralogy and Petrology*, 173(7): 59
- Wilson A H. 2012. A chill sequence to the bushveld complex: Insight into the first stage of emplacement and implications for the parental magmas. *Journal of Petrology*, 53(6): 1123–1168
- Wu Y D, Yang J H, Stagno V, Nekrylov N, Wang J T, Wang H. 2022. Redox heterogeneity of picritic lavas with respect to their mantle sources in the Emeishan large igneous province. *Geochimica et Cosmochimica Acta*, 320: 161–178
- Xiao L, Xu Y G, Mei H J, Zheng Y F, He B, Pirajno F. 2004. Distinct mantle sources of low-Ti and high-Ti basalts from the western Emeishan large igneous province, SW China: Implications for plume–lithosphere interaction. *Earth and Planetary Science Letters*, 228(3–4): 525–546
- Xu Y G, Chung S L, Jahn B M, Wu G Y. 2001. Petrologic and geochemical constraints on the petrogenesis of Permian–Triassic Emeishan flood basalts in southwestern China. *Lithos*, 58(3–4): 145–168
- Xu Y G, He B. 2007. Thick, high-velocity crust in the Emeishan large igneous province, southwestern China: Evidence for crustal growth by magmatic underplating or intraplating. In: *Special Paper 430: Plates, Plumes and Planetary Processes*. Boulder, Colorado, USA: Geological Society of America: 841–858
- Yang S H, Maier W D, Godel B, Barnes S J, Hanski E, O'Brien H. 2019. Parental Magma Composition of the Main Zone of the Bushveld Complex: Evidence from in situ LA-ICP-MS Trace Element Analysis of Silicate Minerals in the Cumulate Rocks. *Journal of Petrology*, 60(2):

- 359–392
- Yu S Y, Song X Y, Ripley E M, Li C S, Chen L M, She Y W, Luan Y. 2015. Integrated O-Sr-Nd isotope constraints on the evolution of four important Fe-Ti oxide ore-bearing mafic-ultramafic intrusions in the Emeishan large igneous province, SW China. *Chemical Geology*, 401: 28–42
- Yuan Q, Namur O, Fischer L A, Roberts R J, Lü X B, Charlier B. 2017. Pulses of plagioclase-laden magmas and stratigraphic evolution in the upper zone of the bushveld complex, South Africa. *Journal of Petrology*, 58(8): 1619–1643
- Zhang Z C, Mahoney J J, Mao J W, Wang F S. 2006. Geochemistry of picritic and associated basalt flows of the western Emeishan flood basalt province, China. *Journal of Petrology*, 47(10): 1997–2019
- Zhang Z C, Mao J W, Saunders A D, Ai Y, Li Y, Zhao L. 2009. Petrogenetic modeling of three mafic-ultramafic layered intrusions in the Emeishan large igneous province, SW China, based on isotopic and bulk chemical constraints. *Lithos*, 113(3–4): 369–392
- Zhong H, Hu R Z, Wilson A H, Zhu W G. 2005. Review of the link between the hongge layered intrusion and Emeishan flood basalts, southwest China. *International Geology Review*, 47(9): 971–985
- Zhong H, Yao Y, Hu S F, Zhou X H, Liu B G, Sun M, Zhou M F, Viljoen M J. 2003. Trace-element and Sr-Nd isotopic geochemistry of the PGE-bearing hongge layered intrusion, southwestern China. *International Geology Review*, 45(4): 371–382
- Zhong H, Yao Y, Prevec S A, Wilson A H, Viljoen M J, Viljoen R P, Liu B G, Luo Y N. 2004. Trace-element and Sr-Nd isotopic geochemistry of the PGE-bearing Xinjie layered intrusion in SW China. *Chemical Geology*, 203(3–4): 237–252
- Zhou M F, Arndt N T, Malpas J, Wang C Y, Kennedy A K. 2008. Two magma series and associated ore deposit types in the Permian Emeishan large igneous province, SW China. *Lithos*, 103(3–4): 352–368
- Zhou M F, Chen W T, Wang C Y, Prevec S A, Liu P P, Howarth G H. 2013. Two stages of immiscible liquid separation in the formation of Panzhihua-type Fe-Ti-V oxide deposits, SW China. *Geoscience Frontiers*, 4(5): 481–502
- Zhou M F, Malpas J, Song X Y, Robinson P T, Sun M, Kennedy A K, Leshner C M, Keays R R. 2002. A temporal link between the Emeishan large igneous province (SW China) and the end-Guadalupian mass extinction. *Earth and Planetary Science Letters*, 196(3–4): 113–122
- Zhou M F, Robinson P T, Leshner C M, Keays R R, Zhang C J, Malpas J. 2005. Geochemistry, petrogenesis and metallogenesis of the Panzhihua gabbroic layered intrusion and associated Fe-Ti-V oxide deposits, Sichuan Province, SW China. *Journal of Petrology*, 46(11): 2253–2280

(本文责任编辑: 刘莹; 英文审校: 张兴春)

·亮点速读·

芬诺斯堪迪业地盾的始太古代陆核：古大西洋克拉通的残迹

初始陆核由于容易被后期地壳再循环作用所破坏或被年轻的岩石所遮盖,使得有关太古宙克拉通的初始演化、地壳生长和保存过程等信息难以获取。虽然芬诺斯堪迪业地盾已知最古老的岩石为3.5 Ga,但时常出现的3.7 Ga的继承性和碎屑锆石表明该地盾可能存在一个尚未暴露的更古老陆核。为了揭开这一谜团,来自哥本哈根大学的Peterson A. 及其合作者对流经芬兰中部和西北部的三条主要河流的碎屑锆石进行了U-Pb、O和Lu-Hf同位素分析,并对芬兰中部太古代片麻岩、石英岩和变辉长岩的锆石O和Lu-Hf同位素数据进行了研究。

新获得的数据以及前人的数据中都含有年龄介于3.73~3.08 Ga且谐和度高于95%的锆石颗粒。这些锆石的Th/U和 $^{207}\text{Pb}/^{206}\text{Pb}$ 之间存在正相关

系,且年龄越老的锆石颗粒具有越高的Th/U比值。其中具有最高Th/U比的锆石具有老于3.5 Ga的 $^{207}\text{Pb}/^{206}\text{Pb}$ 年龄,作者从新的数据中识别出了15个老于3.5 Ga锆石颗粒,这些锆石被认为来自风化或埋藏的古火成岩,因而证实芬诺斯堪迪业地盾确实存在始太古代地壳。在 $^{176}\text{Hf}/^{177}\text{Hf}$ vs. $^{207}\text{Pb}/^{206}\text{Pb}$ 关系图上,这些锆石数据点形成了一个近水平的分布,表明年轻的锆石是古老锆石发生铅丢失的结果,而Hf同位素并未发生改变。在 $\epsilon_{\text{Hf}}(t)$ 与年龄关系图中,这些数据点形成了一个陡的演化趋势线,并在3.75 Ga时与球粒陨石演化线相交,反映其来源于一个始太古代的陆核。作者发现,年轻锆石的Hf同位素总是沿着3.7~3.6 Ga锆石地壳演化趋势线变化,意味着在芬诺斯堪迪业地盾存在一个以前未被识别的

太古宙陆核。这一发现大大增加了在全球各地太古宙地体中发现更多太古宙陆核的可能性,突显了陆核在大陆地壳生长中的重要作用。芬诺斯堪迪业地盾太古宙陆核的同位素特征与格陵兰岛同时代的岩石相似,表明芬诺斯堪迪业地盾和北大西洋克拉通早在始太古宙就曾经紧密相连。

以上成果发表在国际著名地学期刊 **Geology**: Peterson A, Waight T, Kemp A I S, Whitehouse M J, Valley J W. 2024. An Eoarchean continental nucleus for the Fennoscandian Shield and a link to the North Atlantic craton. *Geology*, 52: 171–175, <https://doi.org/10.1130/G51658.1>

(袁超 编译)



柏中杰, 1983年生, 中国科学院地球化学研究所研究员。主要从事幔源基性岩浆作用及成矿研究在峨眉山大火成岩省钒钛磁铁矿大规模成矿的关键控制因素及动力学机制, 以及弧岩浆硫化物饱和和历史制约斑岩成矿潜力等方面取得一系列重要研究成果。获国家自然科学基金优秀青年基金资助, 入选中国科学院“西部青年学者”, 中国科学院青年创新促进会成员, 获第19届侯德封矿物岩石地球化学青年科学家奖和中国有色工业科学技术二等奖(第六)。负责中国科学院西部之光A类项目、中国科学院青促会项目等课题。以第一作者/通信作者在*Geochimica et Cosmochimica Acta*、*Journal of Petrology*、*Economic Geology*、*Mineralium Deposita*、*Chemical Geology*、*American Mineralogist*等学术期刊上发表SCI论文十余篇。



王华建, 1984年生, 中国石油勘探开发研究院高级工程师。主要从事烃源岩地球化学研究。针对油气勘探新区新领域的生油气物质基础这一关键科学问题, 从地球系统演化角度研究有机质富集生烃的多元相互作用, 在中元古界原生油气资源前景、富铀烃源岩层系的油气生成机理、大庆油田页岩油的生物母源和富集环境等方面取得了多项创新成果。近年来主持国家自然科学基金项目3项, 参与国家重点研发计划、油气重大专项、基金委重点项目等5项, 以第一/通讯作者发表SCI/EI收录论文25篇, 铀辐射有机质生油的论文被*Energy & Fuels*期刊选为封面文章, 获中国石油天然气集团有限公司科技进步特等奖、一等奖各1次。2022年获中国矿物岩石地球化学学会第19届侯德封青年科学家奖。



胡清扬, 1987年出生, 北京高压科学研究中心研究员。主要研究地球深部的水和含水矿物。发现地球深部条件下稳定存在的二氧化铁(*Nature* 2016), 据此主导了一系列水与矿物反应生成超氧化物的工作(*PNAS* 2017, *NSR* 2021), 地球深部造氧假说的主要提议人, 为地球早期大氧化事件提供一种深部成因。研究矿物在高温高压下的相变(*Nat. Comm.* 2015, *JACS* 2022)和储水性能(*PNAS* 2020, *EPSL* 2022), 发现含水矿物的金属化(*Sci. Bull.* 2022)和超离子态转变(*Nat. Geosci.* 2021, *Sci. Adv.* 2023), 依此探索水在地球深部示踪机制。发表SCI学术论文75余篇、SCI他引2000余次, 获19届侯德封矿物岩石地球化学青年科学家奖, GRC Van Valkenburg奖, MRE青年科学家奖, 国际晶体学会青年科学家奖, 入围第二届“科学探索奖”。